J. Am. Ceram. Soc., 70 [10] C-248-C-252 (1987)

Fatigue Crack Propagation in Transformation-Toughened Zirconia Ceramic

R. H. DAUSKARDT, W. YU, AND R. O. RITCHIE

Materials and Chemical Sciences Division, Lawrence Berkeley Laboratory, and Department of Materials Science and Mineral Engineering, University of California, Berkeley, California 94720

Fatigue crack propagation under tension-tension loading is observed in a transformation-toughened partially stabilized zirconia (PSZ) ceramic containing 9 mol% MgO. Such subcritical crack growth behavior is demonstrated to be cyclically induced, based on a comparison with behavior under sustained loading (at the maximum load in the fatigue cycle) and at varying cyclic frequencies. Crack extension rates, which are measured as a function of the cyclic stress intensity range ΔK over the range 10^{-10} to 10^{-6} m/cycle, are found to be load ratio dependent and to show evidence of fatigue crack closure, similar to behavior in metals. Cyclic crack growth rates are observed at ΔK levels as low as 3 MPa·m$^{1/2}$ and are typically many orders of magnitude faster than reported data on environmentally assisted, subcritical crack growth in PSZ under sustained-load conditions.

IT HAS long been the general perception that ceramics do not suffer significant degradation by fatigue.[1-3] Accordingly, other mechanisms of subcritical crack growth, primarily involving environmentally assisted cracking processes under monotonic loading, have received far more attention.[4-7] Of late, however, there has been increasing interest in possible mechanisms of cyclic crack propagation as viable modes of subcritical crack extension in brittle materials,[7-11] although unequivocal demonstrations of fatigue effects are not common.[1]

The refuted existence of true cyclic crack propagation effects in conventional monolithic ceramics has been based primarily on the very limited crack tip plasticity apparent in these materials.[1] However, where other mechanisms of local inelastic deformation prevail, or where unloading induces additional fracture phenomena, the notion of fatigue in ceramics clearly becomes more acceptable. For tension-tension and tension-compression loading, several such mechanisms have been suggested, including the deformation and lateral cracking of crack surface asperities on unloading,[1] tensile opening from the wedging action of asperities[1] or corrosion/reaction products[12] between the crack walls, friction-induced heating at the crack tip,[8] and environmentally assisted cracking processes.[8,12] In addition, fatigue cracking has recently been reported in polycrystalline alumina ceramics under far-field cyclic compression loading.[11]

In ceramics toughened by crack tip shielding mechanisms, employing, for example, dilatant zones around the crack arising from in situ phase transformation or microcracking phenomena,[13,14] the resulting nonlinear stress-strain response suggests the strong possibility of fatigue effects. Although evidence for such behavior in "shielded" ceramics has been observed in bend bars subjected to applied cyclic compressive loading,[15] there is little information on corresponding cyclic crack growth under more conventional tension-tension loading.

It is the prime objective of this note to demonstrate that such cyclic crack growth can occur in transformation-toughened ceramics under tension-tension loading and furthermore that such behavior occurs at stress intensities below, and at crack velocities far above, that commonly reported[5-7] for subcritical crack advance induced by environmental mechanisms.

Experimental Procedure

Precipitated partially stabilized zirconia (PSZ), containing 9 mol% MgO, was selected for the present study as it has been extensively characterized with respect to its transformation-toughening behavior.[13,16-18] Approximately 6% by volume of this material undergoes a stress-induced martensitic transformation, although up to 40% can transform in the high-stress fields near a crack tip.[18] The microstructure consists of cubic ZrO grains, 50 μm in diameter, containing lens-shaped tetragonal precipitates of maximum dimensions 300 nm.[17]

Uniaxial tensile properties indicate a tensile strength of 450 MPa and a Young's modulus of 208 GPa. The material displays marked resistance curve toughness behavior, characteristic of significant crack tip shielding, with an initiation fracture toughness of 3 MPa·m$^{1/2}$ (for an initial crack length of approximately one grain diameter) and a maximum fracture toughness of 5.5 MPa·m$^{1/2}$. Extensive microstructural and mechanical property evaluation on this material have been described elsewhere.[13,16-18]

Fatigue crack propagation studies were conducted on long (>3 mm) through-thickness cracks in 3-mm-length compact C(T) specimens, tested in controlled room air (22°C, 45% relative humidity) using automated electro-servo-hydraulic testing machines. Initiation of a precrack was facilitated by a wedge-shaped starter notch. The cyclic frequency, ν, of the applied stress intensity range ($\Delta K = K_{max} - K_{min}$, where K_{max} and K_{min} are the maximum and minimum stress intensities in the fatigue cycle) was varied between 1 and 50 Hz (sine wave) and the load ratio ($R = K_{min}/K_{max}$) between 0.10 and 0.46. Crack growth rates over the range $\sim 10^{-10}$ and 10^{-6} m/cycle were determined under both manual and computer-controlled K-decreasing and K-increasing conditions (normalized K gradient set at 0.80 mm^{-1} (Ref. 19)). Crack lengths were continuously monitored, with a resolution typically better than 5 μm, by employing an electrical resistance technique[20] on thin (1- to 6-μm-thick) metal foils, which were either bonded or evaporated onto the specimen surface. Simultaneous measurement of the extent of fatigue crack closure[21,22] was achieved using strain gauges mounted on the back surface of the C(T) samples. Using this technique,[23] the stress intensity at closure, K_{cl}, defined at first contact of the fracture surfaces on unloading, is determined from the load corresponding to the first deviation from linearity of the elastic compliance curve. A schematic illustration of these techniques is shown in Fig. 1. Fatigue data are presented in the form of both crack growth rate per cycle, da/dN, and crack velocity (with respect to time), $da/dt = \nu(da/dN)$, as a function of either the applied maximum stress intensity, K_{max}, or the cyclic stress intensity range, ΔK.

Fracture surfaces were examined in the scanning electron microscope (SEM). Crack path profiles were studied using optical microscopy on appropriate polished surfaces perpendicular to the fracture surface.

Results

Results illustrating rates of fatigue crack propagation da/dN in PSZ are presented as a function of the applied stress intensity range ΔK in Fig. 2. The majority of data pertains to a load ratio of 0.10 at a cyclic frequency of 50 Hz, although additional results, at load ratios of 0.15, 0.31 and 0.46 and frequencies of 1 and 10 Hz, are included for comparison. It is apparent that, over the wide range of growth rates studied, propagation rates are a power-law function of the stress intensity range, exhibiting a growth law of the form $da/dN \propto \Delta K^m$, identical with that observed during fatigue in metals.[24] However, whereas the exponent m in metals is typically of the order of 2 to 4 in this regime,[24,25] growth rates in the ceramic are far more sensitive to ΔK, with m values

CONTRIBUTING EDITOR — A. H. HEUER

Received March 31, 1987; revised copy received May 18, 1987; approved May 28, 1987.

Supported by the Director, Office of Energy Research, Office of Basic Energy Sciences, Materials Sciences Division, U.S. Department of Energy, under Contract No. DE-AC03-76SF00098.

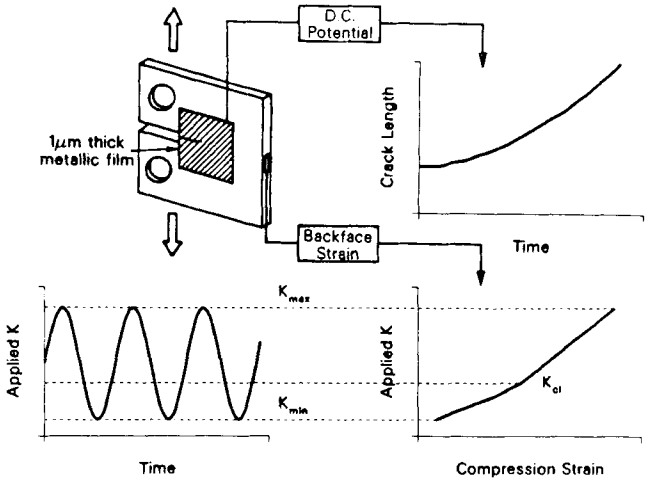

Fig. 1. Schematic illustration of experimental techniques used to continuously monitor crack length and the stress intensity, K_{cl}, at fatigue crack closure.

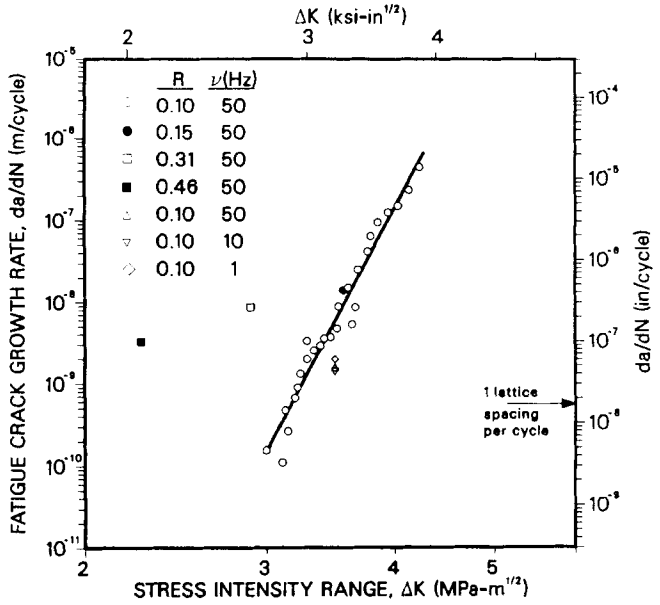

Fig. 2. Variation of fatigue crack propagation rate, da/dN, with applied stress intensity intensity range, ΔK, for PSZ(MgO) ceramic, tested in room-temperature air (45% relative humidity) at a load ratio R of 0.10 and a cyclic frequency of 50 Hz. Data for varying load ratio (0.10 to 0.46) and cyclic frequency (1 to 50 Hz) are included for comparison.

approaching 24. In addition, a marked dependence on load ratio is also apparent. The actual crack growth equation at $R=0.10$, determined from Fig. 2 using regression analysis, is given in units of

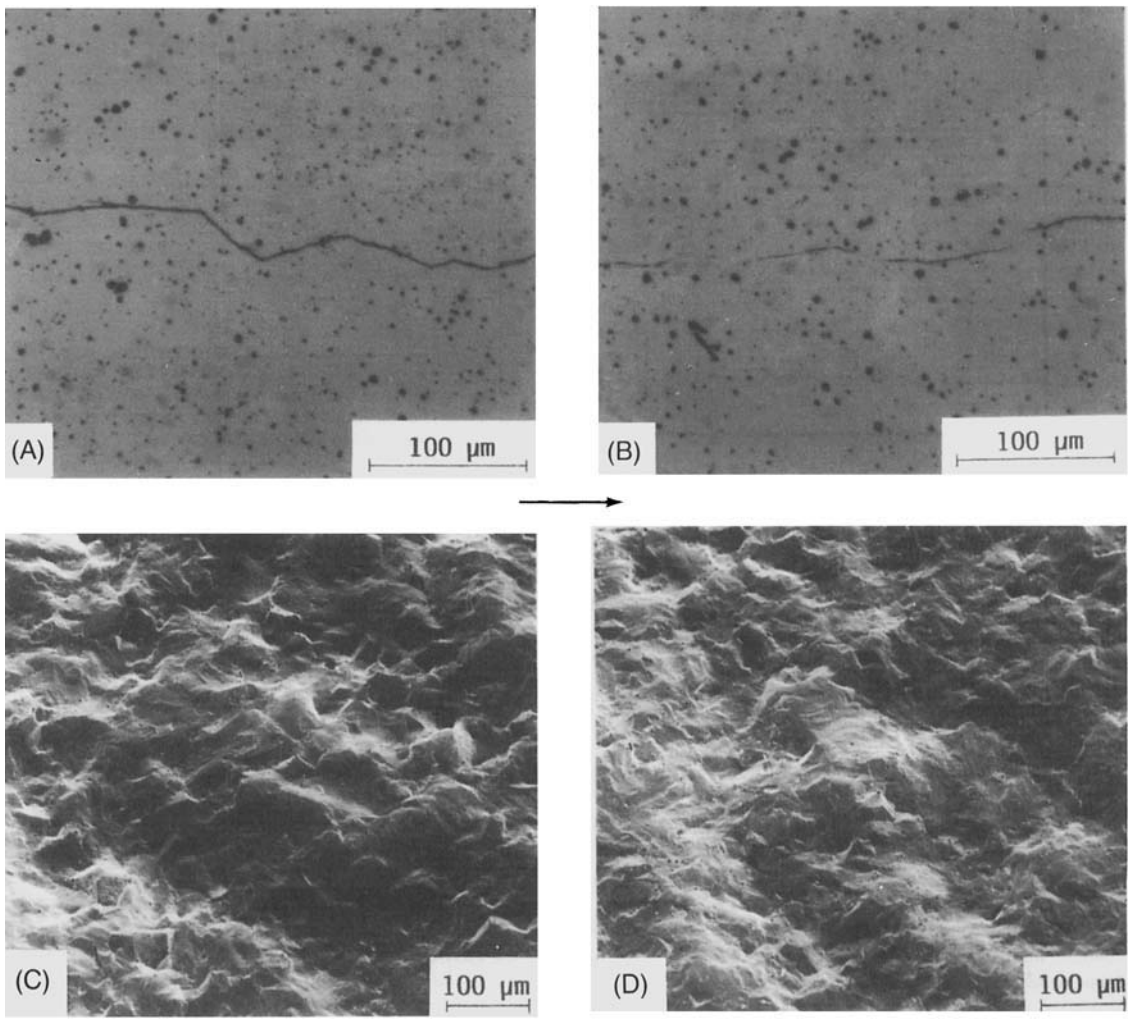

Fig. 3. Fractography of crack growth in PSZ(MgO): optical micrographs of the fatigue crack path, showing (*A*) crack deflection and (*B*) crack bridging immediately behind the crack tip; scanning electron micrographs showing predominantly transgranular fracture surfaces associated with both (*C*) cyclically and (*D*) monotonically loaded cracks. Arrow indicates general direction of crack growth.

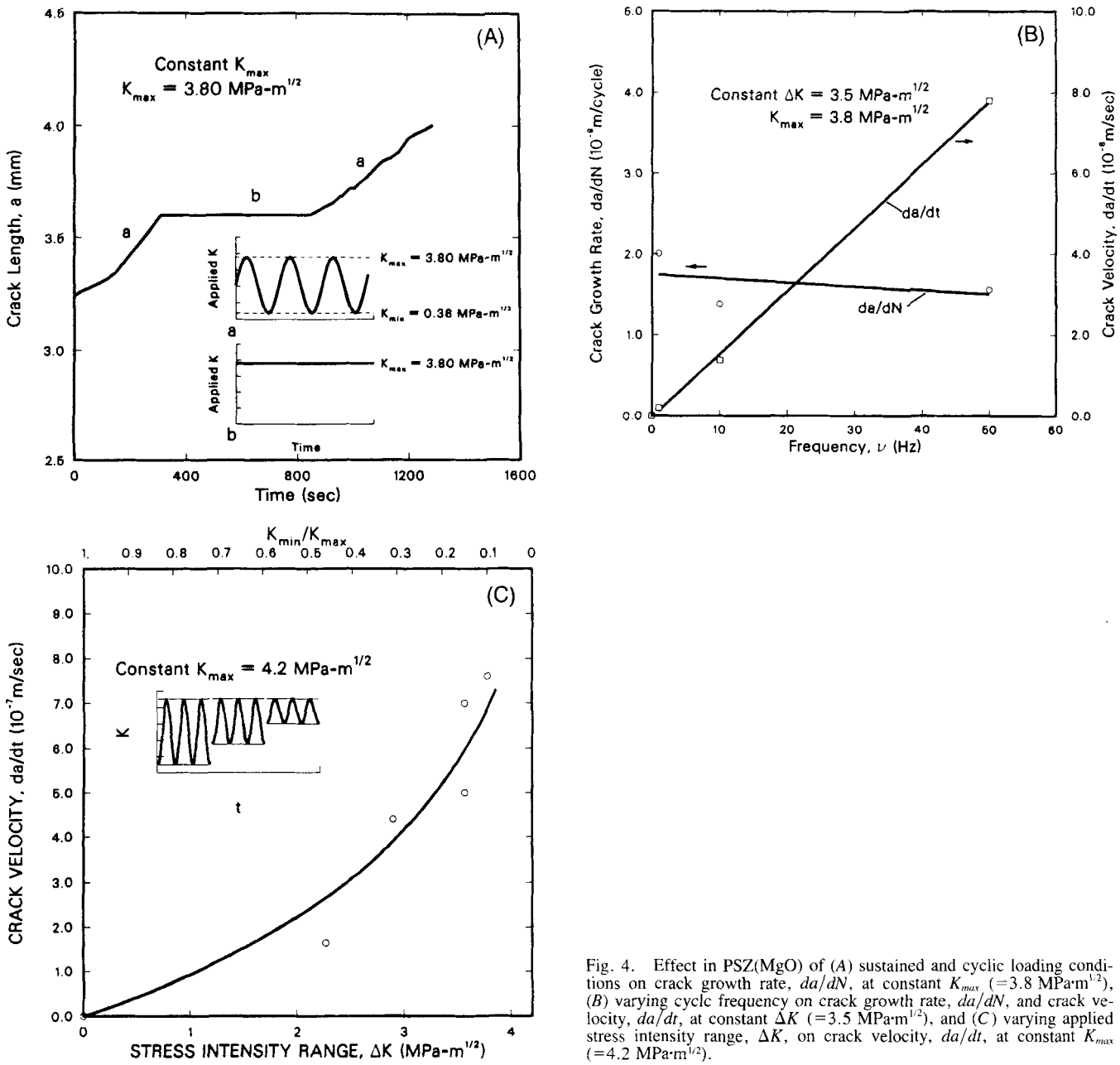

Fig. 4. Effect in PSZ(MgO) of (*A*) sustained and cyclic loading conditions on crack growth rate, da/dN, at constant K_{max} (=3.8 MPa·m$^{1/2}$), (*B*) varying cycle frequency on crack growth rate, da/dN, and crack velocity, da/dt, at constant ΔK (=3.5 MPa·m$^{1/2}$), and (*C*) varying applied stress intensity range, ΔK, on crack velocity, da/dt, at constant K_{max} (=4.2 MPa·m$^{1/2}$).

m/cycle and MPa·m$^{1/2}$ by

$$da/dN = 6.31 \times 10^{-22} (\Delta K)^{24} \quad (1)$$

Optical micrographs of the fatigue crack path in Figs. 3(*A*) and (*B*) show significant crack deflection and evidence of crack bridging just behind the crack tip. SEM examination of the corresponding crack surfaces revealed a transgranular fracture morphology, nominally similar to that obtained under monotonic loading conditions (Figs. 3(*C*) and (*D*)). Although striations have been reported for a glass-ceramic during cyclic contact loading[26] and are commonly seen during the fatigue of metals,[27] no evidence was found in the present study of striations or crack arrest markings in PSZ.

Whereas the data in Fig. 2 apparently show a clear fatigue effect, in view of past skepticism over fatigue in ceramics, it is necessary to demonstrate unequivocally that the crack growth observed is cyclically induced and that other subcritical cracking mechanisms are not responsible. To this end, three separate sets of experiments were conducted (Fig. 4), as described below.

Sustained Load Behavior

To show that the observed crack growth was not merely a result of sustained load cracking at maximum load, crack extension was monitored with (a) the stress intensity cyclically varied between K_{max} and K_{min} and (b) the stress intensity held constant at the same value of K_{max}. This procedure was periodically repeated during the entire range of growth rates; a typical result is shown in Fig. 4(*A*). It is apparent that, whereas crack extension proceeds readily under cyclic loading conditions (region *a*), upon removal of the cyclic component by holding at the same K_{max} (region *b*), no crack growth was detectable.

Influence of Cyclic Frequency

The frequency dependence of rate of crack advance was examined, at a constant ΔK of 3.5 MPa·m$^{1/2}$, for cyclic frequencies of 1, 10, and 50 Hz (Fig. 4(*B*)). For the range of frequencies tested, crack growth rates per cycle, da/dN, were effectively constant and frequency independent, whereas crack velocities with respect to time, da/dt, increased linearly.

Influence of Stress Intensity Range

Rates of fatigue crack propagation in metals are generally more dependent on the range of stress intensity, rather than the mean or maximum levels.[24] To examine this effect in the ceramic, tests were performed at a constant K_{max} (equal to 4.2 MPa·m$^{1/2}$) with increasing K_{min}. Results, in the form of crack velocity, da/dt, as a function of ΔK or the ratio K_{min}/K_{max} shown in Fig. 4(*C*), clearly indicate a

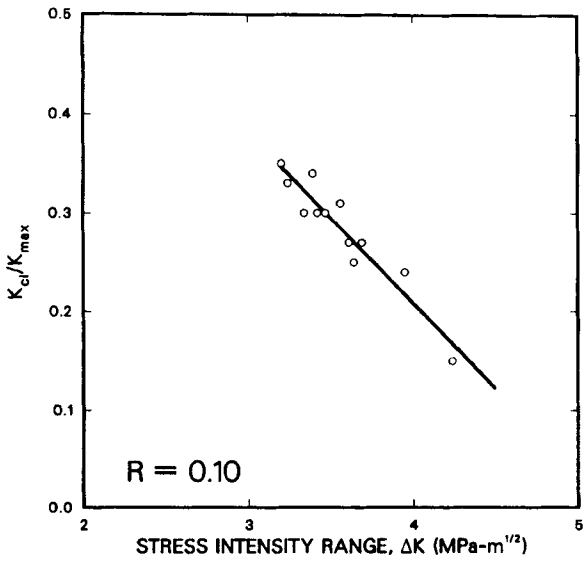

Fig. 5. Experimentally measured variation of fatigue crack closure in PSZ(MgO), corresponding to cyclic crack growth rate data at $R=0.10$ in Fig. 2. Results, based on back-face strain compliance measurements, show the ratio of closure to maximum stress intensity, K_{cl}/K_{max}, as a function of the applied stress intensity range, ΔK.

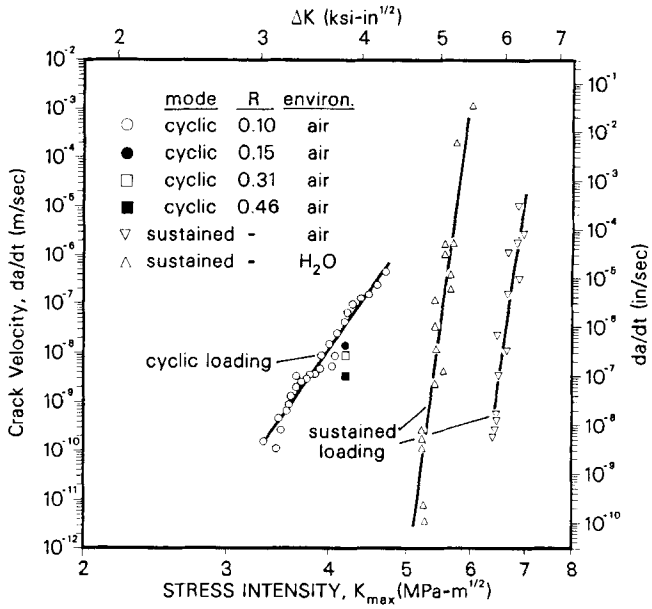

Fig. 6. Subcritical crack growth behavior in PSZ(MgO) showing a comparison of cyclic crack velocities, da/dt, from the present study with sustained-load cracking data of Becher[6,7] for 55% relative humidity air and distilled water. Note how fatigue-induced crack growth is much faster than environmentally assisted crack growth under monotonic loading conditions.

marked effect of decreasing crack velocities with decreasing stress intensity range at constant K_{max}.

Discussion

The above results provide persuasive evidence of true cyclic crack growth in PSZ. Crack growth rates display a dependency similar to that of metals on mechanical factors such as frequency, load ratio, and ΔK, although the sensitivity to the latter two factors is clearly far greater in the ceramic. Moreover, crack advance is associated with several mechanisms of crack tip shielding, which act to reduce the local "crack driving force." In addition to transformation toughening in PSZ, the fatigue cracks show evidence of crack deflection and crack bridging (Fig. 3), and fatigue crack closure involving physical contact between mating crack surfaces.[21,22] The variation in crack closure, as shown by the back-face strain measurements of K_{cl} in Fig. 5, is similar to that seen in metals at low (near-threshold) stress intensities, where closure is developed primarily by corrosion debris or asperities which act as wedges inside the crack.[22] In view of the deflected nature of cyclic crack paths in the ceramic (Fig. 3), it would seem likely that the wedging by fracture surface asperities (roughness-induced closure) is the predominant closure mechanism in PSZ.

It is not feasible in this note to elucidate the precise mechanisms of fatigue in transformation-toughened PSZ. Clearly detailed microstructural studies are required to assess the effect of cyclic loading on such factors as (i) the nature of the inelastic deformation, (ii) the extent of phase transformation, (iii) any concomitant changes in the transformed zone shape which may modify the degree of shielding, and (iv) the changes in the (intrinsic) toughness of material from cyclic damage accumulation mechanisms, such as microcrack formation at particle/matrix interfaces, ahead of the crack tip.

It is apparent, however, that the cyclic crack growth occurs at stress intensities far below, and at crack velocities substantially above, that required for environmentally induced monotonic crack advance in PSZ ceramics. Comparison with Becher's sustained-load cracking data on a similar 7.2 mol% MgO PSZ, tested in 55% relative humidity air and in distilled water,[6,7] indicates fatigue crack growth at stress intensities as low as 3 MPa·m$^{1/2}$, and cyclic crack velocities to be some 8 orders of magnitude faster, at $K_{max}=5$ MPa·m$^{1/2}$, than corresponding rates under monotonic loading (Fig. 6). On the basis of these data, it would appear that nonconservative estimates of subcritical crack extension and serious overestimates of life may result if damage-tolerant predictions in PSZ ceramics are based solely on sustained-load cracking and toughness behavior.

Conclusions

Based on a study of subcritical crack growth under tension-tension fatigue loading in partially stabilized zirconia (PSZ), containing 9 vol% MgO, the following conclusions can be made:

(1) Fatigue crack propagation under tension-tension loading in transformation-toughened PSZ ceramic is unequivocally demonstrated and is shown to be governed by a power-law function of the applied stress intensity range, ΔK, with an exponent of 24.

(2) Akin to behavior in metals, cyclic crack growth rates are found to show similar dependencies on cyclic frequency, load ratio, and ΔK level, although the sensitivity to the latter two factors is far greater in the ceramic.

(3) Cyclic crack growth is predominantly transgranular, with evidence of crack tip shielding by crack deflection, crack bridging (close to the crack tip), and fatigue crack closure presumably arising from crack surface asperity wedging. Akin to near-threshold fatigue behavior in metals, the effect of such closure diminishes with increasing ΔK.

(4) Cyclic crack growth is found to occur at stress intensities far below, and at crack velocities up to 8 orders of magnitude above, that reported for environmentally assisted sustained-load crack growth rates. Such observations may have serious implications for damage-tolerant life predictions in transformation-toughened ceramics.

Acknowledgments

The authors thank Dr. David B. Marshall for supplying the PSZ material, and Dr. Rowland M. Cannon for several helpful discussions.

References

[1] A. G. Evans, "Fatigue in Ceramics," *Int. J. Fract.*, **16** [6] 485–98 (1980).

[2] A. G. Evans and M. Linzer, "High Frequency Cyclic Crack Propagation in Ceramic Materials," *Int. J. Fract.*, **12** [2] 217–22 (1976).

[3] A. G. Evans and E. R. Fuller, "Crack Propagation in Ceramic Materials under Cyclic Loading Conditions," *Metall. Trans.*, **5** [1] 27–33 (1974).

[4] S. M. Wiederhorn, E. R. Fuller, and R. Thomson, "Micromechanisms of Crack Growth in Ceramics and Glasses in Corrosive Environments," *Met. Sci.*, **14** [4] 450–58 (1980).

[5]L.-S. Li and R. F. Pabst, "Subcritical Crack Growth in Partially Stabilized Zirconia (PSZ)," *J. Mater. Sci.*, **15** [11] 2861–66 (1980).
[6]P. F. Becher, "Subcritical Crack Growth in Partially Stabilized ZrO_2(MgO)," *J. Mater. Sci.*, **21** [1] 297–300 (1986).
[7]P. F. Becher, "Slow Crack Growth Behavior in Transformation-Toughened Al_2O_3-$ZrO_2(Y_2O_3)$ Ceramics," *J. Am. Ceram. Soc.*, **66** [7] 485–88 (1983).
[8]D. A. Krohn and D. P. H. Hasselman, "Static and Cyclic Fatigue Behavior of a Polycrystalline Alumina," *J. Am. Ceram. Soc.*, **55** [4] 208–11 (1972).
[9]F. Guiu, "Cyclic Fatigue of Polycrystalline Alumina in Direct Push-Pull," *J. Mater. Sci.*, **13** [6] 1357–61 (1978).
[10]H. N. Ko, "Fatigue Strength of Sintered Al_2O_3 under Rotary Bending," *J. Mater. Sci. Lett.*, **5** [4] 464–66 (1986).
[11]L. Ewart and S. Suresh, "Dynamic Fatigue Crack Growth in Polycrystalline Alumina under Cyclic Compression," *J. Mater. Sci. Lett.*, **5** [4] 774–78 (1986).
[12]L. S. Williams; Ch. 18 in Mechanical Properties of Engineering Ceramics. Edited by W. W. Kriegel and H. Palmour III. Interscience Publishers, New York, 1961.
[13]A. G. Evans and R. M. Cannon, "Toughening of Brittle Solids by Martensitic Transformations," *Acta Metall.*, **34** [5] 761–800 (1986).
[14]A. G. Evans and K. T. Faber, "Crack-Growth Resistance of Microcracking Brittle Materials," *J. Am. Ceram. Soc.*, **67** [4] 255–60 (1984).
[15]S. Suresh, Division of Engineering, Brown University, Providence, RI; personal communication, 1987.
[16]R. H. J. Hannink and M. V. Swain, "Magnesia-Partially-Stabilized Zirconia: The Influence of Heat Treatment on Thermomechanical Properties," *J. Aust. Ceram. Soc.*, **18** [2] 53–62 (1982).
[17]D. B. Marshall, "Strength Characteristics of Transformation-Toughened Zirconia," *J. Am. Ceram. Soc.*, **69** [3] 173–80 (1986).
[18]D. B. Marshall and M. R. James, "Reversible Stress-Induced Martensitic Transformation in ZrO_2," *J. Am. Ceram. Soc.*, **69** [3] 215–17 (1986).
[19]ASTM Standard E 647-86A, "Standard Test Method for Constant-Load-Amplitude Fatigue Crack Growth Rates"; in 1986 ASTM Annual Book of Standards, Vol. 3.01. American Society for Testing and Materials, Philadelphia, PA, 1986.
[20]P. K. Liaw, H. R. Hartmann, and W. A. Logsdon, "A New Transducer to Monitor Fatigue Crack Propagation," *J. Test Eval.*, **11** [3] 202–207 (1983).
[21]W. Elber, "The Significance of Crack Closure"; pp. 230–42 in Damage Tolerance in Aircraft Structures, ASTM STP 486. American Society for Testing and Materials, Philadelphia, PA, 1971.
[22]S. Suresh and R. O. Ritchie, "Near-Threshold Fatigue Crack Propagation: A Perspective on the Role of Crack Closure"; pp. 227–61 in Fatigue Crack Growth Threshold Concepts. Edited by D. L. Davidson and S. Suresh. TMS-AIME, Warrendale, PA, 1984.
[23]R. O. Ritchie and W. Yu, "Short Fatigue Cracks: A Consequence of Crack Tip Shielding"; pp. 167–89 in Small Fatigue Cracks. Edited by R. O. Ritchie and J. Lankford. TMS-AIME, Warrendale, PA, 1986.
[24]P. C. Paris and F. Erdogan, "A Critical Analysis of Crack Propagation Laws," *J. Basic Eng.*, **85** [12] 528–34 (1963).
[25]R. O. Ritchie, "Near-Threshold Fatigue Crack Propagation," *Int. Met. Rev.*, **20** [5–6] 205–30 (1979).
[26]Mei-Chien Lu and A. E. Evans, "Influence of Cyclic Tangential Loads on Indentation Fracture," *J. Am. Ceram. Soc.*, **68** [9] 505–10 (1985).
[27]R. M. N. Pelloux, "Mechanisms of Formation of Ductile Striations," *ASM Trans.*, **62** [1] 281–15 (1969).

J. Am. Ceram. Soc., **70** [10] C-252–C-253 (1987)

Melting Temperatures of Monazite and Xenotime

YASUO HIKICHI* AND TSUYOSHI NOMURA

Department of Materials Science and Engineering, Nagoya Institute of Technology, Gokiso, Showa-ku, Nagoya 466, Japan

The melting temperatures of natural and synthetic monazite and xenotime (rare-earth orthophosphates) were measured, using a heliostat-type solar furnace. The results obtained are as follows: natural monazite from Japan (2057±40°C), synthetic monazite RPO_4 (R=La, 2072±20°C; R=Ce, 2045±20°C; R=Pr, 1938±20°C; R=Nd, 1975±20°C; R=Sm, 1916±20°C), and synthetic xenotime RPO_4 (R=Y, 1995±20°C; R=Er, 1896±20°C).

MONAZITE and xenotime are rare-earth phosphate minerals, and very important ores for sources of rare-earth elements. Ueda *et al.*[1] reported that natural monazite did not melt when fired at 1950°C in air. It seems that the melting temperature of monazite is higher than 1950°C in air. However, no other detailed investigation for the melting temperatures of rare-earth phosphate minerals has been reported. The authors measured the melting temperatures of natural and synthetic monazite and xenotime, using a heliostat-type solar furnace.[2]

Specimens for the measurement of melting temperatures were natural monazite from Nogisawa-mura, Japan (chemical composition: R_2O_3 (R=rare-earth elements), 55.41%; P_2O_5, 26.69%; ThO_2, 11.73%; SiO_2, 2.73%; CaO, 1.11%; Fe_2O_3, 1.49%; Al_2O_3, 0.09%; total, 99.25 wt%), synthetic monazite (monoclinic form RPO_4, R=La, Ce, Pr, Nd, or SM), and synthetic xenotime (tetragonal form RPO_4, R=Y or Er).

The synthetic method is as follows. A solution of RCl_3 (0.05 mol/L, R=La, Ce, Pr, Nd, Sm, Y, or Er) was rapidly added to dilute H_3PO_4 solution (P/R mole ratio 20) and magnetically stirred. The pH of the mixed solution was adjusted to 1.0 with H_3PO_4 or ammonium phosphate solution. The mixed solutions were maintained at 20°C for 3 d and then suction-filtered with a filter paper and washed 5 times with distilled water and finally with acetone. These precipitates were hexagonal form $RPO_4 \cdot 0.5H_2O$ (R=La, Ce, Pr, Nd, or Sm) and weinschenkite-type monoclinic form $RPO_4 \cdot 2H_2O$ (R=Y or Er). When these precipitates were heated to 1000°C in air, they converted to monazite RPO_4 (R=La, Ce, Pr, Nd, or Sm) or xenotime RPO_4 (R=Y or Er), respectively. Monazite and xenotime are stable up to the melting temperatures. Carron *et al.*[3] reported that structures of the rare-earth phosphate compounds were dependent on the kinds of R ions. When the R ion is La, Ce, Pr, Nd, Sm, Eu, or Gd, RPO_4 is a monazite structure, and when the R ion is Tb, Dy, Y, Ho, Er, Tm, Yb, Lu, or Sc, RPO_4 is a xenotime structure. Our results are in agreement with theirs. Chemical compositions of the synthetic monazite or xenotime are almost the same as the theoretical formula, RPO_4. X-ray diffraction patterns of specimens are the same as those of JCPDS card No. 11–556 (natural monazite) or No. 11–254 (natural xenotime), and no other phases are observed in the specimens.

The melting temperature was measured with a heliostat-type solar furnace.[2] In the temperature measurement, a brightness pyrometer is used with a shadowing plate, to obtain the brightness temperature and spectral reflectivity at 0.65 μm from the specular reflection surface of a molten specimen. The spectral emissivity was calculated from reflectivity. Thus the true temperature of the freezing point was estimated from the cooling curves. The brightness temperature of the freezing point was obtained from the cooling curves, which were measured at several points across the sun's

CONTRIBUTING EDITOR—J. A. PASK

Received January 28, 1987; revised copy received April 20, 1987; approved May 8, 1987.
*Member, the American Ceramic Society.